Relations Between Collision Probability, Mahalanobis Distance, and Confidence Intervals for Conjunction Assessment

Relations Between Collision Probability, Mahalanobis Distance and Confidence Intervals for Conjunction Assessment

Dario Modenini,[1] Giacomo Curzi, ,[2] and Alfredo Locarini,[3]

University of Bologna, Forlì 47121, Italy.

Some of the most common metrics for collision risk assessment are the probability of collision, miss distance in Mahalanobis space, and confidence intervals. Sometimes they are used in combination, for example the miss distance is used as a pre-screening method to identify potentially hazardous conjunctions, other times they are used as alternative means, i.e. covariance ellipse overlapping checks are employed instead of computing the probability of collision. In this work, we show that the three risk indexes are intimately connected once a suitable distance is defined. We argue that Mahalanobis miss distance is a proper metric only when the sigma-normalized hardbody size is negligible; we thus investigate the minimum Mahalanobis distance between the hardbody circle and the combined position covariance as an alternative. Its computation is fully analytic, as the most complex operation is finding the roots of a quartic polynomial. When multiplied by the sigma-normalized hardbody radius, such distance provides an upper bound to the collision probability. When used to scale the covariance matrix, it provides the largest confidence interval supporting a non-collision event.

---

[1] Assistant Professor, Department of Industrial Engineering.

[2] Ph.D. Candidate, Department of Industrial Engineering.

[3] Research Fellow, Department of Industrial Engineering.

Accepted version of a manuscipt published on AIAA Journal of Spacecraft and Rockets. DOI: https://doi.org/10.2514/1.A35234.
Editorial version available at: https://arc.aiaa.org/doi/10.2514/1.A35234

Finally, when adopted as an actionable threshold, analytical bounds on the probability of miss detection and of false alarms can be computed.

Nomenclature

A = aspect ratio of the covariance ellipse

$\mathcal{B}$ = combined hardbody circle domain

C = 2x2 combined position uncertainty covariance matrix, km^2

$\boldsymbol{d}$ = miss distance vector, km

$f, \mathcal{N}$ = bidimensional joint Gaussian probability density function

H = Hessian matrix

k = reciprocal of Lagrange multiplier, km^2

$\mathcal{K}_{nc}$ = confidence in non-collision

L = Lagrangian function

$\boldsymbol{m}$, $\boldsymbol{M}$ = absolute extrema points for Mahalanobis distance on the hardbody circumference

m_C = Mahalanobis distance to covariance ellipse C

P = probability

$\boldsymbol{P}$ = primary location

R = combined hardbody radius, km

S = hardbody circle area, km^2

$\boldsymbol{S}$ = secondary location

u = variable for sigma-normalized hardbody radius squared

$\boldsymbol{u}$ = line-of-sight direction

v = variable for Mahalanobis distance squared

$\boldsymbol{x}$ = point on the encounter plane

α = confidence level

φ = phase angle on the hardbody circumference with respect to x axis, rad

Δ = miss distance vector length, km

Accepted version of a manuscipt published on AIAA Journal of Spacecraft and Rockets. DOI: https://doi.org/10.2514/1.A35234.
Editorial version available at: https://arc.aiaa.org/doi/10.2514/1.A35234

λ = Lagrange multiplier, , km^{-2}

σ = standard deviation of position uncertainty, km

θ = angle between covariance ellipse major axis and $\boldsymbol{d}$ vector, rad

Subscripts

c = collision

fa = false alarm

md = miss detection

t = true

thr = threshold

x,y = component along *x,y* axis of the encounter frame

Superscripts

* = extremum point

T = transpose

I.Introduction

Fast pre-screening of collision alerts is used to identify pairs of resident space objects (RSO) that come close enough to be considered potentially hazardous, thus demanding for careful monitoring while approaching the time of closest approach. Often, probability of collision (P_c) is used as a risk metric [1], [2] so that a minimum distance threshold must be determined from the minimum acceptable-probability threshold. This, in turn, requires numerically evaluating a 2D collision integral plus determining an appropriate distance-based threshold [2]. In this respect, screening based on the miss distance expressed in the Mahalanobis space is the most common choice and several numerical or analytical approximations have been developed to relate P_c to Mahalanobis distance, [2]-[6].

Even though collision probability is perhaps the most widely accepted metric, it is also known to suffer from a drawback, named "dilution of probability" [7]. While the predicted collision probability initially increases as the RSOs trajectories uncertainty grows, beyond a certain uncertainty level the collision risk starts decreasing, giving rise to a false safety confidence.

Accepted version of a manuscipt published on AIAA Journal of Spacecraft and Rockets. DOI: https://doi.org/10.2514/1.A35234.
Editorial version available at: https://arc.aiaa.org/doi/10.2514/1.A35234

The countermeasures proposed to this phenomenon are mainly of two kinds [8]. The first is so-called maximum P_c principle [7], stating that, if the positional data are not of sufficient quality so that the outcome of the collision integral computation falls into the dilution region, it is advised using the maximum probability at the onset of dilution, rather than the one predicted from the available data.

The second approach can be called the *ellipse overlap* method [9]: the idea is to enforce (prevent) a certain degree of separation (overlap) between the positional covariance error ellipses, obtained when projecting the problem in the encounter plane. This last concept is closely related to that of confidence regions [10]-[12]: whenever the scaled joint covariance corresponding to a given confidence level, say (1-α), does not intersect the hardbody, then one can state that a *confidence* in non-collision is supported with a (1-α) level. Despite being very intuitive, such an approach leaves open the choice of the required confidence level for non-overlapping ellipses upon which a conjunction can be labelled as safe. In fact, simply setting α equal to the P_c threshold tends to significantly over-estimate the need for remediation actions [8].

In summary, distance thresholding, collision probability, and confidence regions, are three valid alternatives available to spacecraft operators for judging the likelihood of a collision. Despite different works seeking to highlight mutual relations and/or respective advantages/disadvantages between these indexes, [2],[4],[6],[8]-[12], a comprehensive framework connecting the three metrics is still lacking in the literature.

In an attempt to fill such a gap, this work starts from the observation that the miss distance in Mahalanobis space (i.e. Mahalanobis distance) assesses the separation between the *centers* of the RSOs, accounting for their position uncertainties, but regardless of their size. On the other hand, collision probability does actually depend on the size of the spacecraft, represented by the combined hardbody circle, so that one may seek for a more appropriate distance metric. To this end, we propose the *minimum* Mahalanobis distance between a point on the hardbody circumference (centered at the primary) and the secondary. Such a minimum can be computed analytically, as it involves finding the roots of a quartic polynomial. It also features some properties which highlight interesting connections to the remaining two risk metrics. First, the minimum distance is directly related to the highest confidence level in non-collision, i.e. in a miss distance vector not intersecting the hardbody circle. The geometric interpretation is that the point of minimum Mahalanobis distance belongs to one of the scaled covariance ellipses tangent to the circle. Second, by leveraging the concept of bidimensional integral average, the minimum Mahalanobis distance can be shown to provide an upper bound to P_c, when multiplied by the sigma-normalized hardbody area.

Accepted version of a manuscipt published on AIAA Journal of Spacecraft and Rockets. DOI: https://doi.org/10.2514/1.A35234.
Editorial version available at: https://arc.aiaa.org/doi/10.2514/1.A35234

The main contribution of this work is therefore twofold: on one side, it investigates the minimum Mahalanobis distance as a suitable metric to account for the size of the RSOs involved in a conjunction; on the other side, it attempts to provide a unified view on Mahalanobis distance, P_c and confidence intervals. Furthermore, since the involved relations do not rely on simplifying assumptions, they hold for any range of relevant conjunction parameters.

The paper is organized as follows. Section II reviews some preliminaries of collision probability computation in the encounter plane and its relationship with Mahalanobis distance, focusing on the approximations involved, and range of validity. Section III presents the minimum Mahalanobis distance index, its geometric interpretation, and its connections to the confidence in non-collision and collision probability. In Section IV, the performance of the minimum Mahalanobis distance as a risk index is assessed under two aspects, namely i) by computing bounds for the miss detection and false alarm probabilities as a function of the adopted action threshold, and ii) by comparing the required computational burden against that of common P_c computation methods. Finally, conclusions are drawn in Section V.

II. Preliminaries on collision probability

In this work, we consider the so-called short-term encounter framework for analyzing a conjunction event, whose standard assumptions are briefly recalled hereafter [1], [2]. Once two objects are identified to have relevant collision risk, they are considered at the time of closest approach, such that their relative motion can be assumed rectilinear. The positional errors are both assumed to be zero-mean, Gaussian and uncorrelated. The relative velocity at closest approach is assumed sufficiently large to ensure a short encounter time and constant positional covariance, with the velocity uncertainty not contributing to position uncertainty.

Within such assumptions, the probability of collision can be computed from the integral of a two-dimensional Gaussian probability density function (pdf), this last being obtained by combining the three-dimensional pdf of the relative position and marginalizing on the plane perpendicular to the relative velocity vector at closest approach (encounter plane). Although other approaches exist for computing the probability of collision without relying on dimensionality reduction, it has been recently shown [13] that the 2-D simplification performs quite well when compared to the 3-D P_c counterpart, apart from certain pathological cases.

Call $\mathcal{N}(\boldsymbol{d}, C)$ the two dimensional distribution, where $\boldsymbol{d}$ is the mean relative position (i.e. the miss-distance vector) having length Δ, and C is the combined covariance matrix. We consider the geometry represented in Figure 1, with

Accepted version of a manuscipt published on AIAA Journal of Spacecraft and Rockets. DOI: https://doi.org/10.2514/1.A35234.
Editorial version available at: https://arc.aiaa.org/doi/10.2514/1.A35234

the combined hardbody centered on the primary space object (***P***), which defines the origin of the coordinate system. The probability density is instead centered on the secondary space object (***S***). For ease of computations, we adopt within said plane a reference frame that is defined by the principal axes of the combined covariance ellipse, with the *x* axis aligned to the major axis, and call θ the angle between that axis and $\boldsymbol{d}$ vector. Such a frame can always be obtained starting from any other *x*-*y* axes definition upon diagonalization of the covariance matrix.

The collision probability is the integral of the two-dimensional probability density over the combined hardbody area $\mathcal{B}$ and reads:

$$P_c = \frac{1}{2\pi|C|^{1/2}} \iint_{\mathcal{B}} e^{-\frac{1}{2}(\boldsymbol{x}-\boldsymbol{d})^T C^{-1}(\boldsymbol{x}-\boldsymbol{d})}\, dxdy. \tag{1}$$

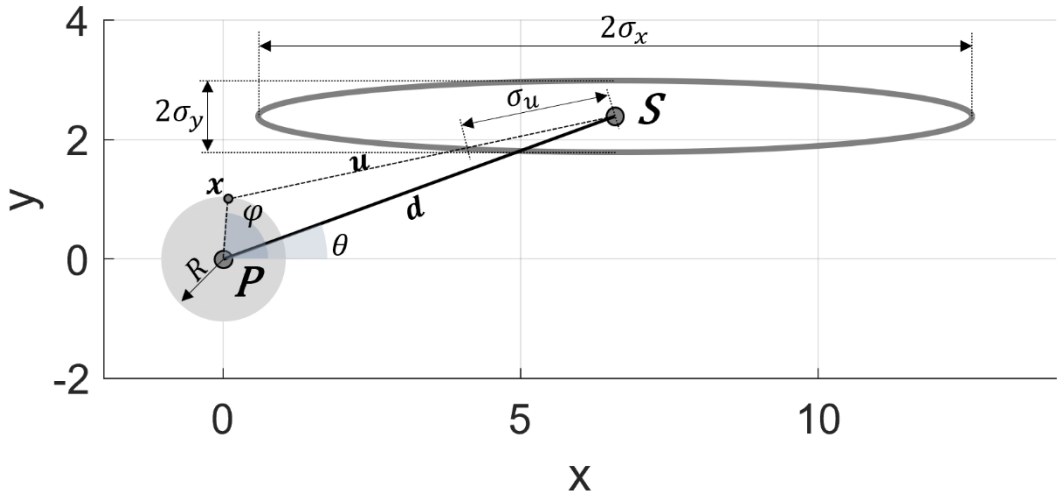

Figure 1 Encounter geometry adopted in this work for 2D collision probability analysis.

The choice of the principal covariance axes for the reference frame leads to a diagonal *C* as in:

$$C = \begin{bmatrix} \sigma_x^2 & 0 \\ 0 & \sigma_y^2 \end{bmatrix}. \tag{2}$$

The exponent in the integrand of Eq. (1) can be recognized as the squared Mahalanobis distance of point $\boldsymbol{x}$ to the covariance ellipse centered at $\boldsymbol{d}$:

$$m_C^2(\boldsymbol{x}) = (\boldsymbol{x}-\boldsymbol{d})^T C^{-1}(\boldsymbol{x}-\boldsymbol{d}) \tag{3}$$

Accepted version of a manuscipt published on AIAA Journal of Spacecraft and Rockets. DOI: https://doi.org/10.2514/1.A35234.
Editorial version available at: https://arc.aiaa.org/doi/10.2514/1.A35234

Expressing the collision integral as a function of the Mahalanobis distance allows highlighting some useful geometric properties. Indeed, Mahalanobis distance can be interpreted as the distance to the ellipse center measured in number of standard deviations along the line-of-sight direction $\boldsymbol{u} = (\boldsymbol{x} - \boldsymbol{d})$, i.e:

$$m_C = \frac{\|\boldsymbol{u}\|}{\sigma_u} \tag{4}$$

where σ_u can is computed as:

$$\sigma_u = \frac{\|\boldsymbol{u}\|}{\sqrt{\boldsymbol{u}^T C^{-1} \boldsymbol{u}}} \tag{5}$$

so that the ellipse points defined by C are, by definition, those points having Mahalanobis distance to the center equal 1. Similarly, it can be also interpreted as the scale factor of the homothetic ellipse passing for the given point, since:

$$(\boldsymbol{x} - \boldsymbol{d})^T C^{-1} (\boldsymbol{x} - \boldsymbol{d}) = m_C^2 \Rightarrow (\boldsymbol{x} - \boldsymbol{d})^T (m_C^2 C)^{-1} (\boldsymbol{x} - \boldsymbol{d}) = 1 \tag{6}$$

A known characteristic of Eq. (1) is that, for fixed object size and miss distance, the variation of P_c as a function of position uncertainty has a maximum (Figure 2): to the left of such maximum, larger positional uncertainties lead to higher P_c, to the right of such maximum instead, increasing uncertainty reduces P_c. Since trajectory uncertainty is driven by the amount and quality of tracking data, the apparent implication is that more/better data would not just reduce the risk of collision, but in some cases increase it. This phenomenon is known as *dilution of probability*. A visual representation is found in Figure 2 for the illustrative example of isotropic covariance matrix ($\sigma_x^2 = \sigma_x^2 = \sigma^2$) and Δ/R=100.

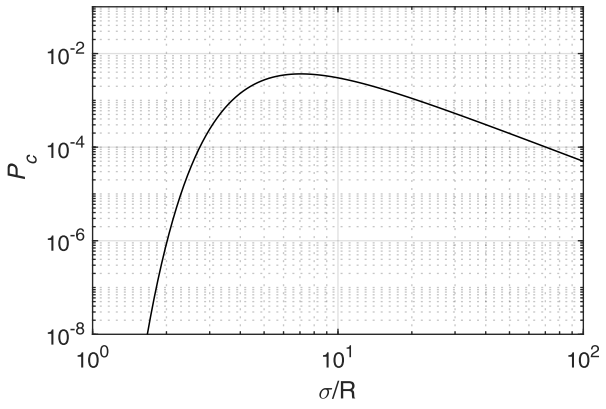

Figure 2 P_c as a function of the inverse sigma-normalized hardbody radius for Δ/R=100 and isotropic covariance.

Accepted version of a manuscipt published on AIAA Journal of Spacecraft and Rockets. DOI: https://doi.org/10.2514/1.A35234.
Editorial version available at: https://arc.aiaa.org/doi/10.2514/1.A35234

The area integral in Eq.(1) shall be evaluated numerically and different methods have been proposed to this end through the years, leveraging quadrature [14],[15], or series expansion [1],[16],[17]. An early and widespread approximation is the one developed by Chan [1], which transforms the two-dimensional Gaussian pdf to a one-dimensional Rician pdf. To this end, he rescaled the problem in the encounter frame to circularize the covariance-error ellipse thereby making the projected combined object footprint an ellipse. He then replaced this object ellipse with a circle of equivalent area. This way, the probability of collision reduces to the integral of an isotropic Gaussian function over a disk shifted from its peak, which is the cumulative function of a non-central χ^2 distribution with two degrees of freedom. Finally, Chan approximated the Rician pdf integral as a series expansion, leading to the following equation:

$$P_c = e^{-v/2} \sum_{m=0}^{\infty} \frac{v^m}{2^m m!} \left(1 - e^{-u/2} \sum_{k=0}^{m} \frac{u^k}{2^k k!} \right), \tag{7}$$

where:

$$\begin{aligned} v &= m_C^2(\mathbf{0}) = \frac{d_x^2}{\sigma_x^2} + \frac{d_y^2}{\sigma_y^2}, \\ u &= \frac{R^2}{|C|^{1/2}} = \frac{R^2}{\sigma_x \sigma_y}. \end{aligned} \tag{8}$$

Direct numerical solution of Eq. (1) or of its approximation via Eqs. (7), allows predicting the collision integral for various ranges of the relevant parameter in the encounter plane. When collision probability is used in screening thousands of pairs of resident space objects for potential conjunction events, clearly simpler analytical formulas are preferable for computational speed. As an alternative, screening method based on distance have been proposed, as discussed in the next section.

A. Distance thresholding for collision screening

Given that a collision occurs when the miss vector lies inside the hardbody radius, it makes sense to search for a screening method based on the miss distance itself. Indeed, several distance-based index can be considered for collision risk assessment, which have been reviewed e.g. in [5]. Most often, the chosen index is the miss distance expressed in Mahalanobis space, which is obtained from Eq.(3) evaluated at $\boldsymbol{x} = \mathbf{0}$.

To select an appropriate distance threshold, one approach is that of relating Mahalanobis miss distance to collision probability and then setting the distance threshold based on a desired P_c threshold [2],[4],[6]. In [2], an analytical approximation that relates maximum probability to a miss-distance threshold was developed, relying on Chan's

Accepted version of a manuscipt published on AIAA Journal of Spacecraft and Rockets. DOI: https://doi.org/10.2514/1.A35234.
Editorial version available at: https://arc.aiaa.org/doi/10.2514/1.A35234

circularization method. Some years later, Alfano and Oltrogge [4] provided a relationship between Mahalanobis space and P_c in the same framework of the Rician approximation, which was there solved numerically (in contrast to the earlier analytical approximation) to derive bounding values for false alarms (Type I errors) and missed alarms that result in a collision (Type II errors). More recently, authors of [6] assumed that the combined hardbody size is small with respect to the covariance, so that the probability integral can be approximated by the value of the *pdf* at the hardbody center multiplied by the circle surface *S*:

$$P_C \cong Sf(0,0) = S\frac{e^{-m_C^2(\mathbf{0})/2}}{2\pi|C|^{1/2}} = \frac{R^2}{2|C|^{1/2}}\, e^{-m_C^2(\mathbf{0})/2}, \tag{9}$$

In doing so, a direct relation between the miss distance and probability of collision is obtained, which was claimed to be sufficiently accurate when the hardbody radius is less than 0.2 times σ_y. The advantage of this approach is that it yields to a simple analytic formula relating the probability of detecting an impending collision to an action threshold based on the P_c.

Despite approximate analytical formulas are very useful to provide physical insight, the errors introduced by the intrinsic simplifications shall be carefully assessed and the range of applicability identified. As an example, we consider three encounter geometries representative of real conjunctions taken from ESA Kelvins' Collision Avoidance Challenge dataset[4]. The values of the combined hardbody radius and miss distance are readily available from the dataset. Since the remaining encounter parameters ($R/|C|^{1/4}$, σ_x, σ_y, ϑ) are not, they have been estimated starting from the primary-to-secondary relative position and velocity at closest approach, and the respective 3D position covariance matrices, after assuming a circular orbit for the primary. Table 1 displays the evaluation of the collision probability for those encounters, comparing the numerical solution of Eq.(1) using Patera's method [14], and the approximate predictions using Eq. (7) and Eq. (9).

Results suggest that the accuracy of both methods degrades when the encounters feature high $R/|C|^{1/4}$ and covariance aspect ratios, which is to be expected, as the involved approximations assume either of them to be small. Note that we do not seek to question the usefulness of the above approximations, which surely remains in many practical applications. Rather, we wish to motivate our quest for a distance metric which is more appropriate when the effect of the sigma-normalized size of the combined hardbody cannot be neglected.

[4] Retrievable at: https://kelvins.esa.int/collision-avoidance-challenge/data/.

Accepted version of a manuscipt published on AIAA Journal of Spacecraft and Rockets. DOI: https://doi.org/10.2514/1.A35234.
Editorial version available at: https://arc.aiaa.org/doi/10.2514/1.A35234

Table 1: Comparison between different approximations of P_c for three encounters

Input parameters			
Dataset ID	1595	293	1875
$R/\|C\|^{1/4}$	0.088	0.344	0.190
σ_x (km)	0.300	0.179	0.289
σ_y (km)	0.013	0.010	0.010
R (km)	5.550×10^{-3}	1.486×10^{-2}	1.044×10^{-2}
Δ (km)	0.112	0.609	0.637
ϑ (°)	18.2	-0.45°	-2.57
P_c			
Eq. (1)	1.291×10^{-4}	1.632×10^{-4}	7.183×10^{-5}
Chan's method	1.148×10^{-4}	2.229×10^{-4}	4.032×10^{-5}
Ref. [6]	1.142×10^{-4}	1.949×10^{-4}	3.852×10^{-5}

B. Bounds on collision probability, integral average, and minimum Mahalanobis distance

Consider the situation depicted in Figure 1, and let $\boldsymbol{M}$, $\boldsymbol{m}$ be the points on the hardbody circumference having respectively the largest and smallest Mahalanobis distance to the covariance ellipse center. These will also be extremal points for the joint Gaussian *pdf* $f(x,y)$ within $\mathcal{B}$, such that:

$$f(M_x, M_y) \leq \frac{1}{S}\iint_{\mathcal{B}} f(x,y)dS \leq f(m_x, m_y), \tag{10}$$

or:

$$Sf(M_x, M_y) \leq P_C \leq Sf(m_x, m_y). \tag{11}$$

Furthermore, since a circle is a bounded and connected domain, any parametric curve $(x(t), y(t)), t \in (0,1)$ connecting (m_x, m_y) and (M_x, M_y) and which lies within $\mathcal{B}$, will include a point $(\bar{x}, \bar{y})$ whose Mahalanobis distance $\bar{m}_C$ to the covariance satisfies the integral average equation:

$$P_C = Sf(\bar{x}, \bar{y}) = \frac{R^2}{2|C|^{1/2}}\, e^{-\bar{m}_C^2/2}, \tag{12}$$

according to the intermediate value theorem. More generally, all points belonging to the scaled covariance ellipse $(\bar{m}_C^2 C)$ and to the hardbody area satisfy Eq. (12). Eq. (12) is a generalization of Eq. (5) in [6], except that here we let $\bar{m}_C^2$ be the distance associated to some point inside the hardbody rather than its center. The two equations would coincide in the limit of small sigma-normalized hardbody ratio, thus suggesting that only within such assumption the Mahalanobis miss distance is a suitable screening method when P_c is used as a risk metric.

Accepted version of a manuscipt published on AIAA Journal of Spacecraft and Rockets. DOI: https://doi.org/10.2514/1.A35234.
Editorial version available at: https://arc.aiaa.org/doi/10.2514/1.A35234

Remark 1. We argue that, if an *approximate* relation between P_c and a distance metric shall be pursued for fast collision screening, so that a threshold on P_c translates into a distance threshold, then the approximation should be based on an upper bound to P_c. This for preventing miss detections due to an underestimated P_c lower than the action threshold when the true P_c is instead higher. The observation above motivates the study of Mahalanobis distance as a means to set bounds on P_c, and the use of the minimum distance between the hardbody and the covariance ellipse as a risk indicator, which is discussed in the next Section.

III.The minimum Mahalanobis distance and confidence in non-collision

Consider the encounter frame depicted in Figure 1. In such a frame, the covariance matrix is diagonal, with corresponding ellipse equation:

$$(\boldsymbol{x}-\boldsymbol{d})^T C^{-1}(\boldsymbol{x}-\boldsymbol{d})-1=0, \tag{13}$$

where:

$$C^{-1}=\begin{bmatrix}\sigma_x^{-2} & 0\\ 0 & \sigma_y^{-2}\end{bmatrix}. \tag{14}$$

According to the prior discussion, we argue that a suitable distance metric could be the minimum Mahalanobis distance between the hardbody circle and the combined position covariance. More precisely, we search for the point on the hardbody circumference $\partial\mathcal{B}=\{\boldsymbol{x}\in\mathbb{R}^2:\boldsymbol{x}^T\boldsymbol{x}-R^2=0\}$ whose Mahalanobis distance to the secondary is the smallest, that is, to the solution of the following constrained minimization problem:

$$\min_{\boldsymbol{x}\in\partial\mathcal{B}}[(\boldsymbol{x}-\boldsymbol{d})^T C^{-1}(\boldsymbol{x}-\boldsymbol{d})] \tag{15}$$

By the method of Lagrange multipliers, the extremal points of Eq. (15) are the unconstrained extrema of:

$$L(\boldsymbol{x},\lambda)=(\boldsymbol{x}-\boldsymbol{d})^T C^{-1}(\boldsymbol{x}-\boldsymbol{d})+\lambda(\boldsymbol{x}^T\boldsymbol{x}-R^2), \tag{16}$$

where λ is the unknown scalar multiplier enforcing $\boldsymbol{x}\in\partial\mathcal{B}$. That is, the points satisfying simultaneously:

$$\begin{aligned}\frac{\partial L}{\partial \boldsymbol{x}}&=C^{-1}(\boldsymbol{x}-\boldsymbol{d})+\lambda\boldsymbol{x}=\boldsymbol{0}\\ \frac{\partial L}{\partial \lambda}&=\boldsymbol{x}^T\boldsymbol{x}-R^2=0.\end{aligned} \tag{17}$$

Since the function to be minimized and the constraint function are both convex, the system is guaranteed to have a solution. This can be easily obtained by solving the first of Eq. (17) for $\boldsymbol{x}$ and substituting into the second, yielding

Accepted version of a manuscipt published on AIAA Journal of Spacecraft and Rockets. DOI: https://doi.org/10.2514/1.A35234.
Editorial version available at: https://arc.aiaa.org/doi/10.2514/1.A35234

to an equation having λ as only unknown. The nature of the extrema depends on the determinant of the Hessian of Eq. (16), also known as (half) bordered Hessian:

$$H(\boldsymbol{x},\lambda)=\begin{bmatrix}0 & x & y\\ x & \sigma_x^{-2}+\lambda & 0\\ y & 0 & \sigma_y^{-2}+\lambda\end{bmatrix}, \tag{18}$$

which reads:

$$|H(\boldsymbol{x},\lambda)|=-\left[x^2\left(\sigma_y^{-2}+\lambda\right)+y^2(\sigma_x^{-2}+\lambda)\right]=-R^2\left(\cos^2(\varphi)\sigma_y^{-2}+\sin^2(\varphi)\sigma_x^{-2}+\lambda\right), \tag{19}$$

where we have used the constraint equation $\boldsymbol{x}\in\partial\mathcal{B}$, calling φ the angle between any extremum point lying on the hardbody circumference and the *x*-axis (see Figure 1). Then, having a two-dimensional state vector and one scalar constraint, the minima and maxima of $L(\boldsymbol{x},\lambda)$ require, respectively:

$$-\left(\lambda+\cos^2(\varphi)\sigma_y^{-2}+\sin^2(\varphi)\sigma_x^{-2}\right)\begin{cases}<0\rightarrow\text{minimum}\\ >0\rightarrow\text{maximum}\end{cases} \tag{20}$$

The suitability of the Mahalanobis distance to the hardbody circumference as a risk indicator is supported by the following

Theorem. Let $\boldsymbol{x}^*$ be a solution of Eq. (17), i.e. an extremum point of m_C^2 on $\partial\mathcal{B}$. Then it is also a point of tangency between $\partial\mathcal{B}$ and the ellipse having matrix $(m_C^2(\boldsymbol{x}^*)C)^{-1}$.

Proof. Assume that $\boldsymbol{x}^*$ is an extremum of $m_C^2(\boldsymbol{x})$. Then, $\boldsymbol{x}^*$ belongs to the ellipse of matrix $(m_C^2(\boldsymbol{x}^*)C)^{-1}$, see Eq.(6). The outward normal to $\partial\mathcal{B}(\boldsymbol{x}^*)$ is clearly $\boldsymbol{x}^*$ (the normal to a circumference point passes through its center). On the other hand, the normal to the ellipse follows from the gradient of Eq. (13) as $(m_C^2(\boldsymbol{x}^*)C)^{-1}(\boldsymbol{x}^*-\boldsymbol{d})$. However, from the first of Eq. (17) these two normals are parallel or anti-parallel (depending on the sign of λ) meaning that the circle and the homothetic covariance ellipse are tangent in $\boldsymbol{x}^*$.

Remark 2. One might define other distance metrics which accounts for the finite size of the combined hardbody. Other reasonable choices could be the closest point of the covariance ellipse to the circumference (which is also the closest point to the origin), or the Mahalanobis distance to the circumference along the miss distance vector. In the former case, one searches the minimum of the Euclidean distance between any point of the ellipse to the origin [18] and then subtracts the hardbody radius. In the latter, one would instead consider the ratio $\frac{\Delta-R}{\sigma_\Delta}$. Here instead, we are searching for the point on the circumference having the smallest Mahalanobis distance to the center of the ellipse. Figure 3 highlights the difference between these alternatives, where $\boldsymbol{m}$, $\boldsymbol{e}$, and $\boldsymbol{l}$, are the points on the circumference respectively having the smallest Mahalanobis, Euclidean and line-of-sight distance to the covariance ellipse.

Accepted version of a manuscipt published on AIAA Journal of Spacecraft and Rockets. DOI: https://doi.org/10.2514/1.A35234.
Editorial version available at: https://arc.aiaa.org/doi/10.2514/1.A35234

Despite being geometrically meaningful, neither the Euclidean nor the line-of-sight distance would exhibit direct connections to the maximum confidence in non-collision and to the upper bound of collision probability as offered by the minimum Mahalanobis distance.

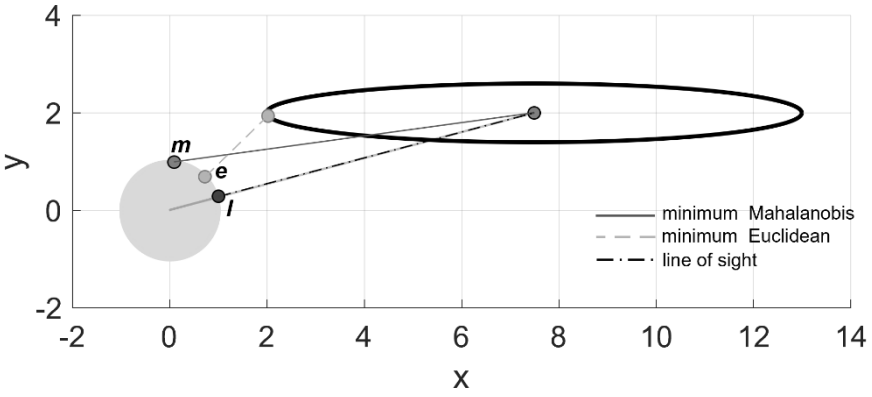

Figure 3 Alternative distance metrics between covariance ellipse and hardbody circle.

A. Solutions to the extrema points of the hardbody Mahalanobis distance

The first of Eqs. (17) can be solved for $\boldsymbol{x}$ as a function of the miss vector components $d_x = \Delta\cos(\theta), d_y = \Delta\sin(\theta)$, indicating such solution with $\boldsymbol{x}^* = [x \quad y]^T$ yields:

$$x = \frac{d_x k}{k + \sigma_x^2} = \frac{\Delta\cos(\theta)\, k}{k + \sigma_x^2} \quad y = \frac{d_y k}{k + \sigma_y^2} = \frac{\Delta\sin(\theta)\, k}{k + \sigma_y^2}. \tag{21}$$

Note that in Eq. (21) we set as unknown $k = \lambda^{-1}$ merely for convenience of the following computations. The tangent of the angle φ from the covariance ellipse major axis to $\boldsymbol{x}^*$ is:

$$\tan(\varphi) = \frac{y}{x} = \tan(\theta)\frac{k + \sigma_x^2}{k + \sigma_y^2}, \tag{22}$$

which is different from θ apart when θ=0°, 90° (i.e. miss vector aligned to one of the ellipse axes). In the isotropic case, clearly $\varphi = \theta$ for any value of θ. Substituting into the circle equation $\|\boldsymbol{x}\|^2/R^2 = 1$, one gets:

$$(d_x k)^2\left(k + \sigma_y^2\right)^2/R^2 + \left(d_y k\right)^2(k + \sigma_x^2)^2/R^2 - \left(k + \sigma_y^2\right)^2(k + \sigma_x^2)^2 = 0, \tag{23}$$

which is a quartic equation in *k*, thus amenable of analytic roots.

It is convenient to express Eq. (23) in the following form:

$$p(k) = ak^4 + bk^3 + ck^2 + dk + e = 0, \tag{24}$$

Accepted version of a manuscipt published on AIAA Journal of Spacecraft and Rockets. DOI: https://doi.org/10.2514/1.A35234.
Editorial version available at: https://arc.aiaa.org/doi/10.2514/1.A35234

$$a = (\Delta/R)^2 - 1,$$
$$b = 2\sigma_y^2[(\Delta/R)^2(\cos^2\theta + \sin^2\theta A^2) - (1 + A^2)],$$
$$c = \sigma_y^4[(\Delta/R)^2(\cos^2\theta + \sin^2\theta A^4) - (1 + A^2)^2 - 2A^2],$$
$$d = -2\sigma_y^6(1 + A^2)A^2,$$
$$e = -\sigma_y^8 A^4,$$

obtained after letting $\sigma_x = A\sigma_y$, A being the covariance aspect ratio. This equation can have (i) two real roots and a couple of complex conjugate roots, or (ii) four real roots[5], corresponding to the cases in which 2 or 4 concentric homothetic ellipses can be found which are tangent to the hardbody circle, see Figure 4 and Figure 5. A full characterization of the nature of the roots is not straightforward, as it involves the study of the cumbersome discriminant of a quartic equation. Some insight can nonetheless be obtained from Descarte's rule of signs, see Appendix.

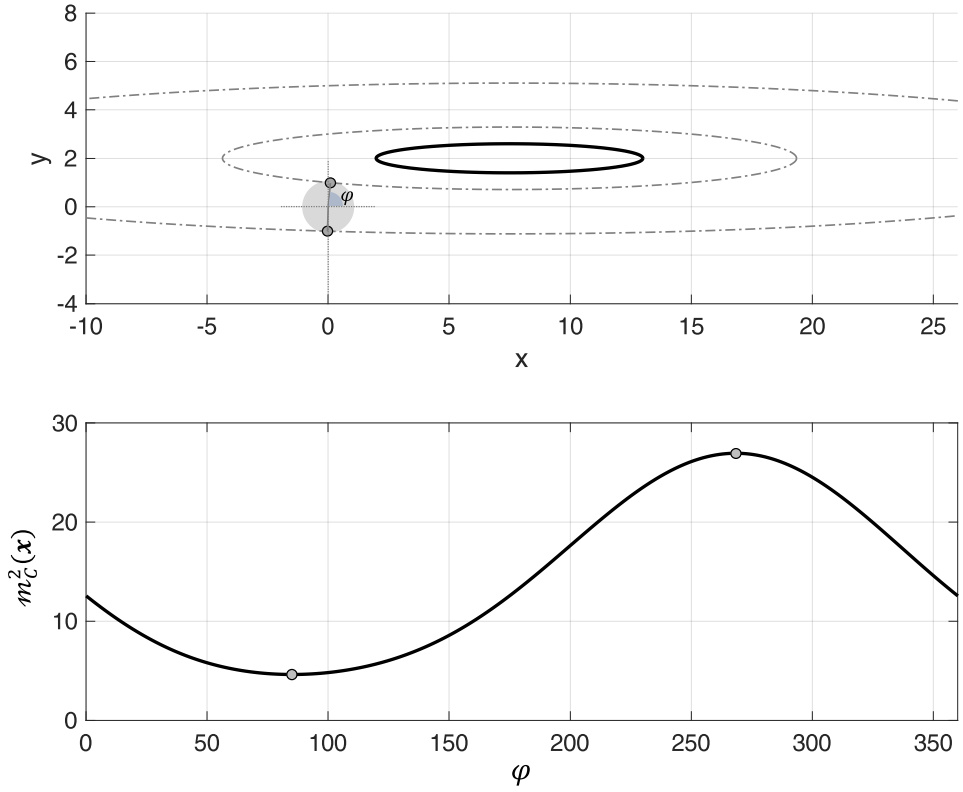

[5] We can discard the possibility of having two couples of conjugate complex roots since Mahalanobis distance on the circumference points is a continuous function over a bounded interval, hence it must possess an absolute maximum and minimum which correspond to two real roots of the quartic equation.

Accepted version of a manuscipt published on AIAA Journal of Spacecraft and Rockets. DOI: https://doi.org/10.2514/1.A35234.
Editorial version available at: https://arc.aiaa.org/doi/10.2514/1.A35234

Figure 4. Type (i) solution featuring two extrema of Eq. (16) (bottom panel) corresponding to two tangent ellipses (top panel).

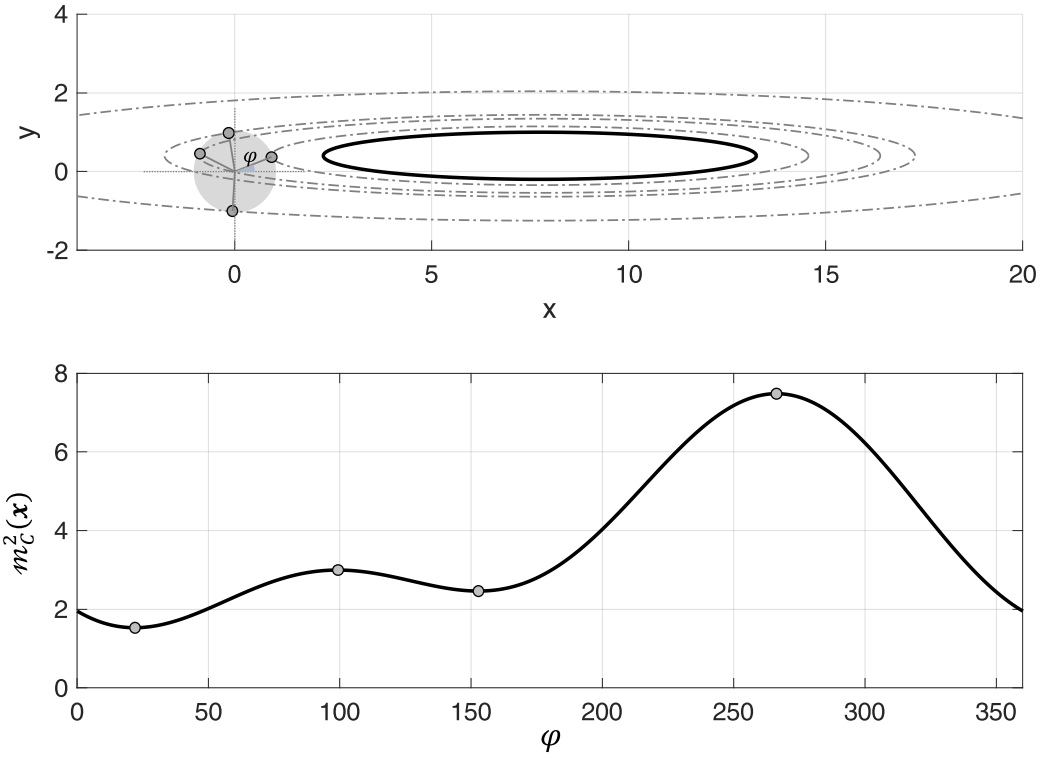

Figure 5. Type (ii) solution featuring four extrema of Eq. (16) (bottom panel) corresponding to four tangent ellipses (top panel) whose centers lie outside the circle.

By substituting Eq. (21) into Eq. (3), the squared Mahalanobis distance at the extrema points can be computed as:

$$m_C^2(\boldsymbol{x}^*) = \left(\Delta\sigma_y\right)^2 \left[\left(\frac{\sin\theta}{k+\sigma_y^2}\right)^2 + \left(\frac{A\cos\theta}{k+A^2\sigma_y^2}\right)^2\right]. \tag{25}$$

It is worth noting that the point of absolute minimum $\boldsymbol{x}^* = \boldsymbol{m}$, belongs to an ellipse which does not overlap the circle, while the absolute maximum $\boldsymbol{x}^* = \boldsymbol{M}$ belongs to an ellipse enclosing the circle. The local extrema, instead, belong to ellipses which partially overlaps the hardbody circle. These observations may also be verified by determining the number of intersection points between the respective ellipse and the hardbody circle using the methods in [19]-[21] based on homogeneous matrix representation.

Finally, we can state the following lemma which completes the solution to the problem of finding the minimum Mahalanobis distance.

Accepted version of a manuscipt published on AIAA Journal of Spacecraft and Rockets. DOI: https://doi.org/10.2514/1.A35234.
Editorial version available at: https://arc.aiaa.org/doi/10.2514/1.A35234

Lemma. Let C represents an ellipse centered outside the hard body circle, $\boldsymbol{x}^*$ be the point associated to the only positive root of Eq. (23), then $\boldsymbol{x}^* = \boldsymbol{m}$ and $m_C^2(\boldsymbol{m})$ is the minimum Mahalanobis distance.

This can be seen by noting that the tangency point having minimum distance is the only one with non-overlapping curves. On the other hand, non-overlapping curves are tangent only when they have antiparallel outward normals, see Figure 4 and Figure 5. From Eq. (17), the only tangency point for which this occurs is the one generated by the positive multiplier $\lambda = k^{-1}$.

From the observation above, we may draw the following

Definition. Let $\boldsymbol{m}$ be the point of absolute minimum for $m_C^2(\boldsymbol{x})$. Then, we call "*confidence in non-collision*" the confidence level $\mathcal{K}_{nc}$ associated to the largest ellipse, non-overlapping the hard-body, i.e.:

$$\mathcal{K}_{nc} = 1 - \alpha^*, \tag{26}$$

where $\alpha^* = e^{-m_C^2(\boldsymbol{m})/2}$.

Remark 3. The definition is well posed, in fact, in [11] it is claimed that a *K*-confidence ellipse not overlapping the hardbody circle supports the non-collision event with *K* probability level. This confidence level has a closed form solution for the two-dimensional case which equates the cumulative function of a central χ^2 distribution having two DoF. Since the covariance matrix $(m_C^2(\boldsymbol{m})C)$ represents the largest ellipse with such a non-overlapping property, the largest confidence in non-collision is indeed Eq. (26).

When the ratio Δ/R becomes smaller than 1, i.e. the ellipse center lies inside the hard body radius, then all the coefficients in Eq. (24) become negative. In such a case, there cannot be positive roots, and we talk of type (iii) solutions. For all the tangency points, the outward normal to the circle and ellipse are parallel, which is the situation depicted in Figure 6. Classifying the critical points originated from such roots is not immediate and not particularly interesting for practical applications, therefore we will not pursue this issue further.

Accepted version of a manuscipt published on AIAA Journal of Spacecraft and Rockets. DOI: https://doi.org/10.2514/1.A35234.
Editorial version available at: https://arc.aiaa.org/doi/10.2514/1.A35234

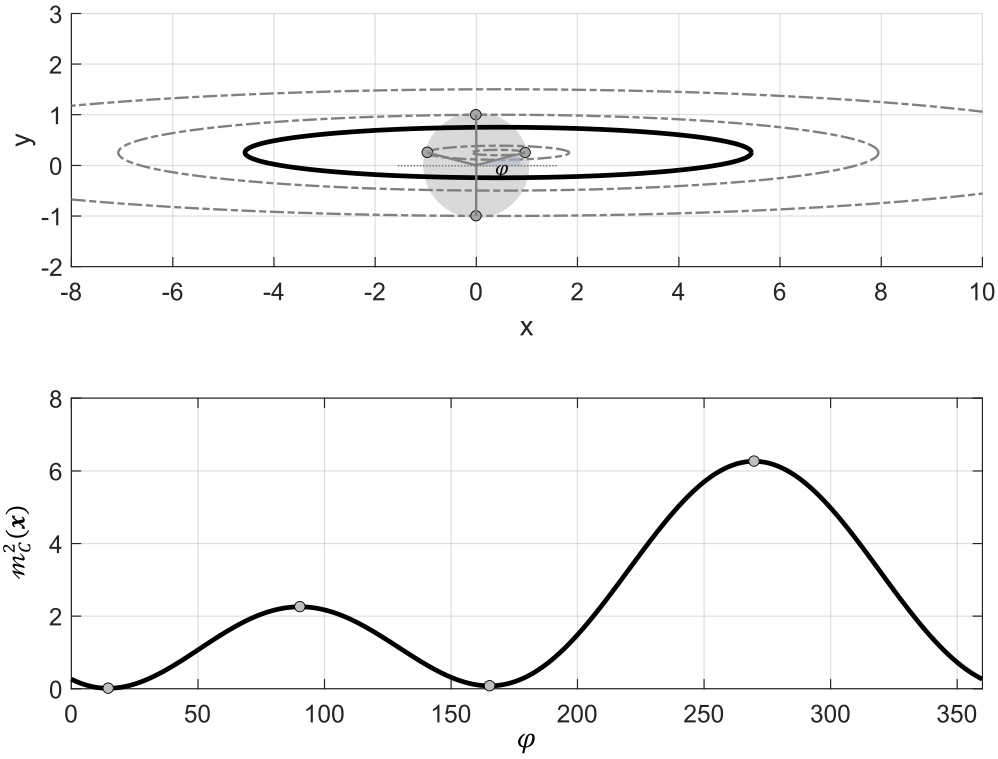

Figure 6. Type (iii) solution featuring four extremal points of Eq. (16) (bottom panel) corresponding to four tangent ellipses (top panel) whose centers lie inside the circle.

B. Relations between P_c and $\mathcal{K}_{nc}$

The absolute extrema points of the Mahalanobis distance give rise to three measures related to collision probability, namely the upper and lower bounds as per Eq.(11), plus the non-collision confidence in Eq. (26). Clearly, if we are confident at $1-\alpha^*$ that we will not collide, the probability that we collide is at most α^*. Meaning that α^* is an upper bound to P_c, even though in most situations such upper bound is very "loose". This is not the case, however, for very close encounters involving large hardbody areas. In such situations, the upper P_c bound computed through Eq.(11) may exceed the unit value, hence violating a fundamental property of a probability measure. Indeed, by prescribing:

$$P_{c,max} = Sf(\boldsymbol{m}) = \frac{R^2}{2\sigma_x\sigma_y} e^{-m_c^2(\boldsymbol{m})/2} = 1, \tag{27}$$

one sees that the $P_c \leq 1$ constrain is violated for sufficiently large sigma-normalized hardbody radius and small Mahalanobis miss distance, i.e. for:

Accepted version of a manuscipt published on AIAA Journal of Spacecraft and Rockets. DOI: https://doi.org/10.2514/1.A35234.
Editorial version available at: https://arc.aiaa.org/doi/10.2514/1.A35234

$$\frac{R^2}{\sigma_x \sigma_y} \geq 2e^{\frac{(d_x - m_x)^2}{2\sigma_x^2} + \frac{(d_y - m_y)^2}{2\sigma_y^2}}. \tag{28}$$

Such occurrence may be avoided by adopting as the upper collision probability bound the minimum between Eq. (27) and $(1 - \mathcal{K}_{nc}) = \alpha^* = e^{-m_C^2(\boldsymbol{m})/2}$, i.e. by setting

$$P_{c,max} = \min(Sf(\boldsymbol{m}), \alpha^*), \tag{29}$$

which leads to the following result for the upper bound on the collision probability as a function of the minimum Mahalanobis distance, $\boldsymbol{m}$:

$$P_{c,max} = \min\left(\frac{R^2}{2\sigma_x \sigma_y}, 1\right) \cdot e^{-\frac{m_C^2(\boldsymbol{m})}{2}} \leq 1. \tag{30}$$

The outcome of the analysis can be finally summarized as follows:

$$\begin{gathered} 0 \leq \frac{R^2}{2\sigma_x \sigma_y} \cdot e^{-\frac{m_C^2(\boldsymbol{M})}{2}} \leq P_c \leq \min\left(\frac{R^2}{2\sigma_x \sigma_y}, 1\right) \cdot e^{-\frac{m_C^2(\boldsymbol{m})}{2}} \leq 1, \\ \mathcal{K}_{nc} = 1 - \alpha^* = 1 - e^{-\frac{m_C^2(\boldsymbol{m})}{2}}, \end{gathered} \tag{31}$$

which provides the desired connections between classical Mahalanobis distance, collision probability P_c and confidence bound $\mathcal{K}_{nc}$.

Advocating the use of confidence in non-collision, in place of P_c (or vice-versa) as the preferred risk metric for undertaking mitigation actions is beyond our scopes. Nevertheless, assuming the upper bound on P_c as the index where to put a threshold, we can state that the confidence interval approach is more conservative, since, in most practical cases, the ratio $\frac{R^2}{2\sigma_x \sigma_y}$ is much smaller than 1. Given that action thresholds based on P_c have been already extensively studied in the literature, in the next section the error probabilities resulting from a screening based on minimum Mahalanobis distance will be analyzed only.

IV. Performance of minimum Mahalanobis distance for conjunction screening

A. Error probabilities

A risk metric and its associated action threshold are often evaluated in terms of their probability of generating false alarms and that of not detecting an impending collision. These are sometimes referred to as Type I and Type II errors, respectively [4], [6]. In other words, one shall address: i) given that we are on a collision course, what is the probability (of non-detection) that the given risk metric will be below the action threshold (P_{md}), and ii) what is the probability

Accepted version of a manuscipt published on AIAA Journal of Spacecraft and Rockets. DOI: https://doi.org/10.2514/1.A35234.
Editorial version available at: https://arc.aiaa.org/doi/10.2514/1.A35234

that two non-colliding RSOs will generate an observed miss-distance such that the risk metric will be above the action threshold (P_{fa}). The formalism developed in Section III allows for deriving upper and lower bounds to these error sources when adopting the minimum Mahalanobis distance as an indicator.

To assess the probability of miss detection we may assume that the observed miss vector is drawn from a Gaussian distribution with the measured position covariance C, but centered at the true miss vector $\boldsymbol{d}_t$ within the hardbody circle, call it $f(\boldsymbol{x}; \boldsymbol{d}_t, C)$, for example its center in case of a head-on collision ($\boldsymbol{d}_t = \boldsymbol{0}$). Then we need to compute the probability that the minimum Mahalanobis distance between the observed miss-distance and the hardbody circle is above a given threshold, m_{thr}. For each true miss vector within the hard body circle (i.e. collision), one could potentially compute the miss detection probability by integrating the pdf (centered at the true position) outside the area whose points have $m_C(\boldsymbol{m}) > m_{thr}$. Similarly, given a true miss vector outside the hard body circle, one could compute the false alarm probability by integrating the pdf inside the area whose points have $m_C(\boldsymbol{m}) < m_{thr}$. Since the true miss vector is obviously unknown, we may rather attempt to obtain bounding values for P_{fa} and P_{md} , i.e. their upper and lower bounds.

To this end, we consider worst-case scenarios for P_{fa} and P_{md}, i.e. a slightly missed hit ($\Delta_{true} \rightarrow R^+$) for Type I error, and a glancing collision ($\Delta_{true} \rightarrow R^-$) for Type II error, identified by the secondary lying on ∂B. One such situation is depicted in **Figure 7**, where we set $R = \Delta_{true} = 1$, $\vartheta = 45°$, $m_{thr} = 1$.

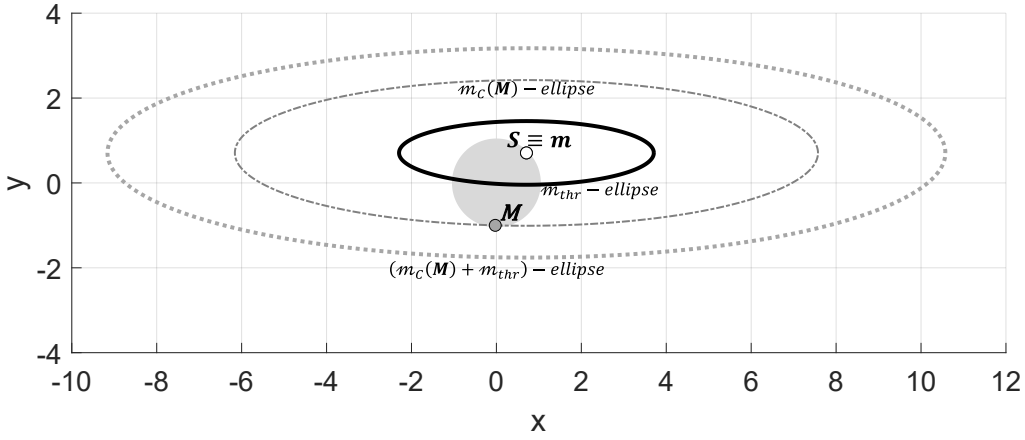

Figure 7. Visual depiction of covariance ellipses for computing bounds on P_{md} and P_{fa}.

Accepted version of a manuscipt published on AIAA Journal of Spacecraft and Rockets. DOI: https://doi.org/10.2514/1.A35234.
Editorial version available at: https://arc.aiaa.org/doi/10.2514/1.A35234

Since we are assuming $\Delta_{true} = R$, clearly the minimum Mahalanobis distance point to the covariance ellipse is $\boldsymbol{m} \equiv \boldsymbol{S} \in \partial B$ and $m_C(\boldsymbol{m}) = 0$. The maximum distance point $\boldsymbol{M}$ is also depicted, which originates an ellipse encompassing the entire hard body circle (see discussion in III.A). As a result, all points that are outside the $(m_C(\boldsymbol{M}) + m_{thr})$ −ellipse would feature a minimum Mahalanobis distance above the action threshold m_{thr}, thus leading to a miss detection. It follows that this integration region is the minimum set of points contributing to miss detection, i.e. it provides a lower-bound to P_{md} once the pdf is integrated on it.

For the upper bound of the miss detection probability, one shall consider the m_{thr}-ellipse. All the points that are inside that ellipse surely lead to a detection, since there is at least one point belonging to ∂B, i.e. the secondary location, whose Mahalanobis distance to the observed point is below the action threshold m_{thr}. This means that all and only the points outside the m_{thr}-ellipse may or may not cause a miss detection. Thus, the integral of the pdf on this region yields a maximum bound to the miss detection probability.

Similar arguments allow deriving bounds on P_{fa}. Since all points inside m_{thr}-ellipse lead to a detection, the confidence level of such ellipse sets a lower bound to P_{fa}. Since all points outside $(m_C(\boldsymbol{M}) + m_{thr})$-ellipse does not provide false alarm, the confidence level of such ellipse sets an upper bound to P_{fa}. In other words, when $\Delta_{true} = R$, $P_{fa} = 1 - P_{md}$.

Lastly, we shall evaluate the integrals of the Gaussian pdf in the respective sets, which amount to the confidence levels of those probability densities at two distinct degrees: one at the ellipse $m_C(\boldsymbol{M}) + m_{thr}$ and the other at the ellipse m_{thr}. These confidence levels are computed in closed form as exponentials (see Remark 3), so that the following bounds on Type I and Type II error probabilities are obtained:

$$\begin{matrix} 1 - e^{-\frac{m_{thr}^2}{2}} < P_{fa} < 1 - e^{-\frac{1}{2}\left(m_{thr} + m_C(\boldsymbol{M})\right)^2} \\ e^{-\frac{1}{2}\left(m_{thr} + m_C(\boldsymbol{M})\right)^2} < P_{md} < e^{-\frac{m_{thr}^2}{2}} \end{matrix} \quad , \frac{\Delta_{true}}{R} = 1 \tag{32}$$

Note, however, that two bounds in Eq.(32) depend on the realization of Δ_{true} through the computation of $m_C(\boldsymbol{M})$. The dependency can be conveniently removed by noting that, out of all points belonging to ∂B, the one for which $m_C(\boldsymbol{M})$ is the largest will provide the highest upper-bound for the false-alarm rate, which in turn occurs at θ=90° (i.e. in correspondence of the ellipse minor axis) for which $m_C(\boldsymbol{M}) = \frac{2R}{\sigma_y} = \frac{2R\sqrt{A}}{|C|^{1/4}}$. On the other hand, the point on ∂B leading to the lowest lower-bound for the probability of miss detection is at the ellipse major axis (θ=0°), when $m_C(\boldsymbol{M})$ is the smallest and equal to $\frac{2R}{\sigma_x} = \frac{2R}{\sqrt{A}|C|^{1/4}}$. In summary:

Accepted version of a manuscipt published on AIAA Journal of Spacecraft and Rockets. DOI: https://doi.org/10.2514/1.A35234.
Editorial version available at: https://arc.aiaa.org/doi/10.2514/1.A35234

$$1 - e^{-\frac{m_{thr}^2}{2}} < P_{fa} < 1 - e^{-\frac{1}{2}\left(m_{thr}+2R/\sigma_y\right)^2} \qquad e^{-\frac{1}{2}(m_{thr}+2R/\sigma_x)^2} < P_{md} < e^{-\frac{m_{thr}^2}{2}} \quad , \frac{\Delta_{true}}{R} = 1 \tag{33}$$

Eq. (33) indicates that for a screening based on the minimum Mahalanobis distance, the threshold m_{thr} defines a lower bound on the probability of false alarms, and an upper bound on the probability of miss detection. On the other hand, upper bound on P_{fa} and lower bound on P_{md} depend also on the sigma-normalized combined hardbody size and on the covariance aspect ratio.

Figure 8 and Figure 9 depict the variation of Eq. (33) as a function of m_{thr} for different values of $\frac{R}{|C|^{1/4}}$ and for aspect ratio *A*=6. The consistency of the above bounds have been tested with Monte Carlo simulations, which confirmed their adequacy. If the minimum Mahalanobis distance is to be used as risk indicator, these charts can guide the selection of the action threshold by trading off between the resulting Type I and Type II errors.

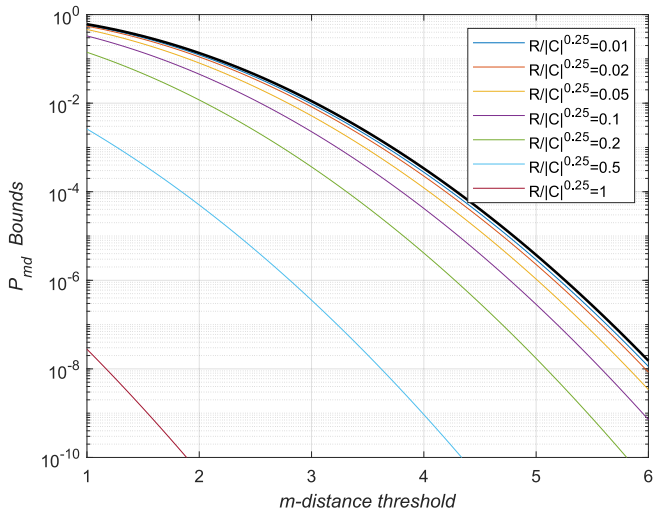

Figure 8. Probability of miss detection vs threshold: upper bound as black bold line, lower bounds displayed for different ratios $R/|C|^{1/4}$.

Accepted version of a manuscipt published on AIAA Journal of Spacecraft and Rockets. DOI: https://doi.org/10.2514/1.A35234.
Editorial version available at: https://arc.aiaa.org/doi/10.2514/1.A35234

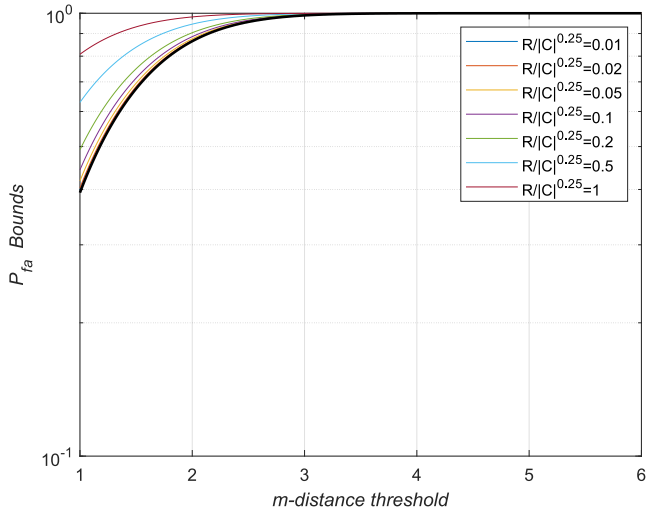

Figure 9. Probability of false alarm vs threshold: lower bound as black bold line, upper bounds displayed for different ratios $R/|C|^{1/4}$.

B. Computational speed

In Section II we motivated the analysis of minimum Mahalanobis distance as a fast screening method for collision risk assessment. However, since its evaluation requires additional computation with respect to a screening based on the miss distance alone, the corresponding burden shall be assessed and compared with that necessary for computing P_c. Such a check is especially important in light of some very efficient computational methods for P_c which have been recently developed, most notably the power series expansions in [16],[17], and the Gauss-Chebyshev quadrature method in [22].

In what follows, we compare the execution times for MATLAB implementations of the minimum Mahalanobis distance computation, along with four methods for computing P_c, namely i) Foster's integral, ii) Patera's method [14], iii) the series expansion of Serra et al. [16], including the first four terms, and iv) Elrod's quadrature technique [22], using Chebyshev polynomials of order 16. The MATLAB codes for methods i) and iv) were taken from NASA Conjunction Assessment Risk Analysis (CARA) open source software[6]. For computing the minimum Mahalanobis distance, we used the method of Ferrari-Cardano [23] to evaluate the only positive root of Eq. (24) through radicals. Execution time was evaluated by replicating 10^5 times a single conjunction event, test-case 1 in CARA Elrod's routine.

[6] https://github.com/nasa/CARA_Analysis_Tools.

Accepted version of a manuscipt published on AIAA Journal of Spacecraft and Rockets. DOI: https://doi.org/10.2514/1.A35234.
Editorial version available at: https://arc.aiaa.org/doi/10.2514/1.A35234

Table 2 displays the different execution times normalized against the fastest method, which were obtained by running the corresponding codes on a Laptop computer equipped with an Intel(R) Core(TM) i7-1185G7 @ 3.00 GHz. Since running multiple instances of the codes indicate some variability of the execution times even in relative terms, these are provided as orders of magnitude. Results indicate that the minimum Mahalanobis distance compares well with P_c in terms of computational burden, although it does not improve in absolute terms with respect to the most efficient P_c calculation through series expansion. It is worth to be noted, however, that the amount of computations required to evaluate $m_C(\boldsymbol{m})$ through the roots of a quartic is fixed for whichever sets of conjunction parameters. On the other hand, convergence of the P_c series expansion up to a desired accuracy level requires a number of terms which depends on the specific problem under consideration. We can thus conclude that minimum Mahalanobis distance may be conveniently adopted for fast conjunction screening.

Table 2: Relative execution times for different algorithms.

P_c				$m_C(\boldsymbol{m})$
Foster [2]	Patera [14]	Serra et al. [16]	Elrod [22]	This work
~1000	~50	~1	~10	~1

V.Conclusion

In this work, we discussed some properties of three commonly employed metrics for assessing the risk of spacecraft collision, namely the collision probability, confidence intervals, and Mahalanobis distance. After reviewing some preliminaries in collision analysis, we have shown the adequacy and utility of the minimum Mahalanobis as a suitable distance when the sigma-normalized hardbody size is not negligible. To this end, we adopt the common assumptions of bi-dimensional analysis in the encounter plane, Gaussian position error distributions and spherical shape of the combined hardbody. By studying the behavior of the Mahalanobis distance function on the hardbody circumference domain, we compute a closed form solution to its extrema, and provide extensive geometric interpretations of the results.

The main findings of this analysis can be summarized as follows:

- the extrema of the Mahalanobis distance computed over the hardbody circumference correspond to the points of tangency of scaled covariance ellipses to the hardbody. Depending on the mutual configuration between

Accepted version of a manuscipt published on AIAA Journal of Spacecraft and Rockets. DOI: https://doi.org/10.2514/1.A35234.
Editorial version available at: https://arc.aiaa.org/doi/10.2514/1.A35234

the ellipse and the circle, the extrema can be either two or four and can be grouped in three families of solutions.

- The largest covariance ellipse non-overlapping the hardbody corresponds to the absolute minimum of the Mahalanobis distance; as such, it provides the largest confidence interval supporting a non-collision event. Such minimum is obtained, in turn, from the only positive root of a quartic equation.
- Bounds to the collision probability can be computed from the absolute extrema of the Mahalanobis distance or, equivalently, from the confidence levels of the corresponding ellipses tangent to the hardbody.
- When minimum Mahalanobis distance is adopted as a screening index, the action threshold and the absolute maximum Mahalanobis distance define confidence ellipses providing upper and lower bounds on the miss detection and false alarm rates.

We do not pretend to break new ground here, since our results are derived from the application of standard tools of geometry and calculus to the problem of collision analysis in the 2D encounter frame. Nonetheless, the material herein is believed to offer a different, hopefully useful, perspective on some commonly employed metrics for collision risk assessment, highlighting a set of properties which hold under little, if any, restrictive assumptions.

Appendix

To study the nature of the roots of Eq. (24) we initially restrict ourselves to the case $\Delta>R$, so that the sign of highest order coefficient a is positive; this is only a mild restriction, since if the estimated miss distance lies inside the hardbody, one can a-priori label the conjunction as dangerous.

The sign of the two lowest order coefficients in Eq. (24) is always negative. The only coefficients that can change sign are the ones of degrees 3 and 2, i.e. b and c. We note that, as the miss distance to hardbody ratio Δ/R grows, b and c are positive. Conversely, they become both negative sign for Δ/R approaching 1. Of all 4 possible sign combinations, the one for which b is negative and c is positive cannot occur, meaning that there is always *one* change of sign among the coefficients of $p(k)$. In fact, assume that $b<0$, then it holds:

$$\left(\frac{\Delta}{R}\right)^2 < \frac{1+A^2}{\cos^2\theta+\sin^2\theta A^2},$$
$$\frac{c}{\sigma_y^4(1+A^2)} = \left[\left(\frac{\Delta}{R}\right)^2 \frac{\cos^2\theta+\sin^2\theta A^4}{1+A^2} - (1+A^2) - \frac{2A^2}{1+A^2}\right] < \left[\frac{\cos^2\theta+\sin^2\theta A^4}{\cos^2\theta+\sin^2\theta A^2} - (1+A^2) - \frac{2A^2}{1+A^2}\right]. \quad (34)$$

Accepted version of a manuscipt published on AIAA Journal of Spacecraft and Rockets. DOI: https://doi.org/10.2514/1.A35234.
Editorial version available at: https://arc.aiaa.org/doi/10.2514/1.A35234

Since $\frac{\cos^2\theta+\sin^2\theta A^4}{\cos^2\theta+\sin^2\theta A^2} \leq A^2$, the right-hand side, and thus c, must cannot be positive. As a result, one can state that both in options (i) and (ii), as defined in Section III.A, there must be only one positive root. It follows that the negative real roots are whether 1, for case (i), or 3, for case (ii). By applying the rule of signs to *p(-k)*, multiple negative roots *may* occur only for

$$\begin{aligned} &b > 0, c < 0, \text{ or} \\ &b < 0, c < 0, \end{aligned} \tag{35}$$

meaning that a necessary condition for having 4 real roots (three of which negative and one positive) is $c<0$, i.e.:

$$(\Delta/R)^2 < \frac{(1+A^2)^2 + 2A^2}{\cos^2\theta + \sin^2\theta A^4}. \tag{36}$$

For a sufficient condition, one shall instead require the discriminant of the quartic to be greater than zero, which however leads to a practically intractable equation.

Funding Sources

This work received no funding.

Acknowledgments

Authors would like to acknowledge the use of the open source NASA CARA program in carrying out the numerical analysis of section IV.B.

References

[1] Chan, F.K. *Spacecraft Collision Probability*, The Aerospace Press, El Segundo, 2008.

[2] Foster, J. L., and Estes, H. S., "A Parametric Analysis of Orbital Debris Collision Probability and Maneuver Rate for Space Debris," NASA JSC-25898, Aug. 1992.

[3] Alfano, S. "Determining a probability-based distance threshold for conjunction screening", *Journal of Spacecraft and Rockets* Vol. 50, No. 3, 2013, pp. 686–690.

[4] Alfano, S., Oltrogge, D. "Probability of Collision: Valuation, variability, visualization, and validity, *Acta Astronautica*," Vol 148, 2018, pp. 301-316, https://doi.org/10.1016/j.actaastro.2018.04.023.

Accepted version of a manuscipt published on AIAA Journal of Spacecraft and Rockets. DOI: https://doi.org/10.2514/1.A35234.
Editorial version available at: https://arc.aiaa.org/doi/10.2514/1.A35234

[5] Phillips, M. “Spacecraft Collision Probability Estimation for Rendezvous and Proximity Operations,” Master of Science Thesis, Utah State University, Logan, Utah, 2012.

[6] Sweetser, T.H., Braun, B.M., Acocella, M. Vincent, M.A. “Quantitative assessment of a threshold for risk mitigation actions,” *Journal of Space Safety Engineering*, Vol 7, No 3, 2020, pp. 318-324, https://doi.org/10.1016/j.jsse.2020.07.009.

[7] Alfano, S. “Relating Position Uncertainty to Maximum Conjunction Probability,” *Journal of the Astronautical Sciences*, Vol. 53, No. 2, 2005, pp. 193-205.

[8] Hejduk M.D., Snow D.E., Newman L.K. “Satellite conjunction assessment risk analysis for ‘dilution region’ events: issues and operational approaches,” In Space Traffic Management Conference, Austin, TX, 26–27 February 2019.

[9] Hejduk M.D., Snow D.E. “Satellite Conjunction “Probability,” “Possibility,” and “Plausibility”: A Categorization of Competing Conjunction Assessment Risk Analysis Paradigms,” *Advances in the Astronautical Sciences*, Vol 171, AAS 19-652.

[10] Balch, M.S. “A corrector for probability dilution in satellite conjunction analysis,” In 18th AIAA Non-Deterministic Approaches Conference, page 1445, 2016. doi: 10.2514/6.2016-1445

[11] Balch, M.S., Martin, R., and Ferson, S., “Satellite Conjunction Analysis and the False Confidence Theorem,” Proceedings of the Royal Society of London, Series A: Mathematical and Physical Sciences, Vol. 475, No. 2227, 2019.

[12] Cunen C., Hjort N.L., Schweder T. “Confidence in confidence distributions!” *Proc. R. Soc. A* 476: 20190781. http://dx.doi.org/10.1098/rspa.2019.0781

[13] Hall, D.T. “Expected Collision Rates for Tracked Satellites,” Journal of Spacecraft and Rockets, Vol. 58 No. 3, May-June 2021.

[14] Patera, R. P., “General Method for Calculating Satellite Collision Probability,” *Journal of Guidance, Control, and Dynamics*, Vol. 24, No. 4, 2001, pp. 716–722.

[15] Alfano, S.. “A numerical implementation of spherical object collision probability,” *Journal of Astronautical Sciences*, Vol. 53, No. 1, 2005, pp. 103–109.

Accepted version of a manuscipt published on AIAA Journal of Spacecraft and Rockets. DOI: https://doi.org/10.2514/1.A35234.
Editorial version available at: https://arc.aiaa.org/doi/10.2514/1.A35234

[16] Serra, R., Arzelier, D., Joldes, M., Lasserre, J. B., Rondepierre, A., & Salvy, B.. Fast and accurate computation of orbital collision probability for short-term encounters. *Journal of Guidance, Control, and Dynamics*, Vol. 39 No. 5 (2016), pp. 1009-1021.

[17] Garcia-Pelayo, R. and Hernando-Ayuso, J. "Series for Collision Probability in Short-Encounter Model." *Journal of Guidance, Control, and Dynamics*, Vol. 39 No. 8 (2016), pp. 1904-1912

[18] Eberly, D. Intersection of Ellipses, Geometric Tools, Redmond WA 98052, 2020. https://www.geometrictools.com/Documentation/IntersectionOfEllipses.pdf

[19] Hill, K. "Matrix-Based EllipseGeometry," *GraphicsGems V*, Academic Press, New York, 1995, pp. 72–77.

[20] Chan, K., "A Simple Mathematical Approach for Determining Intersection of Quadratic Surfaces," American Astronautical Society, AAS Paper 01-358, July–Aug. 2001.

[21] Alfano, S., Greer, M.L. "Determining if two solid ellipsoids intersect," *Journal of Guidance, Control, and Dynamics* Vol. 26, No. 3, 2003, pp. 106–110.

[22] Elrod, C. "Computational Bayesian Methods Applied to Complex Problems in Bio and Astro Statistics." Doctoral Dissertation, Baylor University, July 2019.

[23] Cardano, G., "Ars Magna or the rules of algebra", transl. by Witmer T.R., Dover Publications, 1968.

Accepted version of a manuscipt published on AIAA Journal of Spacecraft and Rockets. DOI: https://doi.org/10.2514/1.A35234.
Editorial version available at: https://arc.aiaa.org/doi/10.2514/1.A35234